

# Design Of A New Comparator Using A Min Algorithm Operating In Low Power

Divya S, PG Scholar, Karpagam University, Coimbaore.  
C. Pandiyarajan, Assistant Professor, Karpagam University, Coimbaore.

**Abstract --A comparator in a low-power 180-nm complementary metal-oxide-semiconductor process using a Cadence Virtuoso tool is presented to operate in the low power with the minimum consumption of the power and with the high throughput with high stable nature. Byutilizing the MIN algorithm this could be achieved. The circuit of a conventional type comparator consisting of two cross-coupled inverters is modified for fast operation even with different GHz at low supply voltages. The advantages of a high-impedance input rail-to-rail output swing robustness against the influence of mismatch in the circuit are considered a important and the architecture is designed in a way that to be operate at the maximum frequency along with the minimum power supply.**

**Index Terms—Comparator, complementary metal-oxide-semiconductor (CMOS) analog circuits, low supply voltage, modified latch, ultradeepsubmicrometer CMOS.**

## INTRODUCTION

In recent years, exploiting near-threshold and subthresholdcircuits has become a major trend in low-power applications,whichputs forward more critical requirements forlow-output-voltage, small-area, and high-efficiency voltagconverters. In modern system on chips (SoCs), multiple power domains are required for various circuit blocks. Fig. 1 shows anexample of an energy-efficient SoC that utilizes energy-efficient near-threshold logic circuits. Targeting low-power applications, theSoC system uses a power supply for the overall system. The 1-V power supply is directly supplied to analog/RF [5] and I/O [8] circuits. In order to utilize near-threshold operation, a voltagconverters is required to generate a 0.5-V power supply from the1-V input for the logic circuits, with 50- $\mu$ A to 10-mA outputcurrent range and high power efficiency. Compared with buck/boost dc-dc converters that use inductors, switched-capacitor voltage converter is a

preferablesolution for low-voltage power supplies because of great potentialto be fully integrated on-chip. The design challenges of the SC voltage converter are: 1) the degrade efficiency atlow output current  $I_{OUT}$ ; and 2) the implementation of 0.5-Vvoltage reference circuit and the power penalty dueto  $V_{REF}$ . In addition, the design of sub-1V is difficult because a typical operates above 1V. In order tosolve the problems, a low-voltage high-efficiency SC voltagconverters with voltag-reference-free pulse-density modulation is proposed for high power efficiency at low  $I_{OUT}$ by both reducing the pulse density and eliminating  $V_{REF}$  [1].

## RELATED WORK

Two major types of conventional comparatortshown in Fig.1. The first type in Fig. 1 usesconstant pulse density for the switch matrix [2]–[4]. Inthis scheme, a non-overlap clock generator is employed to drivethe switch matrix with a fixed clock frequency, as shown inFig. 2. Therefore, it suffers from severe efficiency drop whenoutput current decreases due to excessive clock pulses for smallcurrent demand. Theothertype of conventionalSC voltage converter is attached with the conventional system, which relies on  $V_{REF}$  and a comparatortfor pulse-density modulation (PDM) [5]–[9]. The comparatortcompares the output voltage with the reference voltage to performPDM. Therefore, the pulse density is adjusted accordingto different  $I_{OUT}$ , thus preventing the efficiency drop due toexcessive clock pulses, as shown in Fig.6. The $V_{REF}$  is often omitted in the previous works by simply using anoff-chip voltage supply.

This way, the power loss introduced bythe  $V_{REF}$  is overlooked. Moreover, a sub-1-V voltage referencemay bring extra design complexity to the voltage converter. Therefore, this scheme costs extra power and area, and it makethe circuit design complicated with low power supply voltagdue to the use of an on-chip voltage reference. Fig. 3 show the proposed voltage converter andtiming. The key concept of  $V_{RF}$ -PDM is to replace the reference voltage in Fig. 2 with the past output voltag $V_{OUT}$ , thereby eliminating  $V_{REF}$ . The proposed scheme usestwo sampling clocks, to sample outputvoltag at different times.  $V_{OUT}$  is sampled as  $V_{NOW}$  and $V_{PAST}$  at each falling edge, respectively. Then, sampled voltages  $V_{NOW}$  and  $V_{PAST}$  are compared bya comparator with an offset voltage of  $\Delta V$ . When  $V_{PAST} - V_{NOW}$  is larger than  $\Delta V$ , the comparator output is set to high, and then an expanded pulse signal is generatedas  $SC_{enable}$ . Applying an AND gate to CK and  $SC_{enable}$ , a pulse signal  $SC_{clock}$  is to be generated and then fed tothe non -overlap clock generator to drive the switch matrix. Form the existing this circuit is modified by

adding of the keeper circuit with the 0.07%. 0.07% denotes the usage of the keeper for the voltage references, Read path of the circuit is modified with dynamic multiplexer circuit. Circuit is designed with the low power operating condition with help of above mentioned paper. Responses graphs are created for testing of the circuit. Fig.1. shows the Schematic diagram of the conventional comparator, where the circuit operates without the static power.

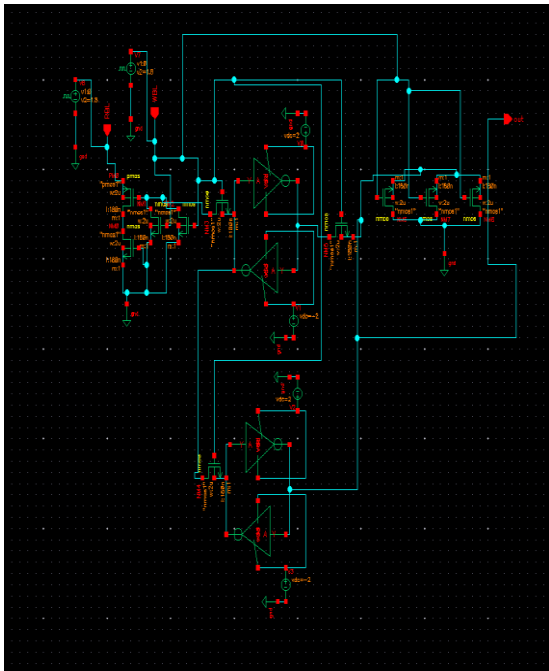


**Fig.1. Schematic diagram of the conventional comparator**

**ADAPTIVE FLOATING-GATE COMPARATOR**

The simple circuit shown in Fig. 2 is built with the conventional comparator built using CMOS transistors with PMOS and NMOS transistors which is implemented using the Virtuoso tool, comprising pre-amplification and regenerative stages for the comparison as well as control and local storage for the adaptation. During normal operation, floating gate transistors and form the input devices of a differential pair and provide local charge storage. Cross-coupled nFET transistors and forms the regenerative elements of the comparator. When the clock signal is high the nFET switch closes and resets the comparators. When low switch is opens and the evaluation phase begins. The “high” bias voltage on transistor during reset determines conductance of the regenerative elements and there by the overall gain and speed of the comparators. With the power-supply  $V_{dd}$  set at the nominal operating voltage of 3 V, there is insufficient electric field between the pFET’s drain and source to produce hot electrons in the channels of and devices. We therefore keep the AFGC’s  $V_{dd}$  at 2.5 V during both normal operation and adaptation. V strengthens source-to-drain electric fields

there by increasing the energy of electrons in the channels.

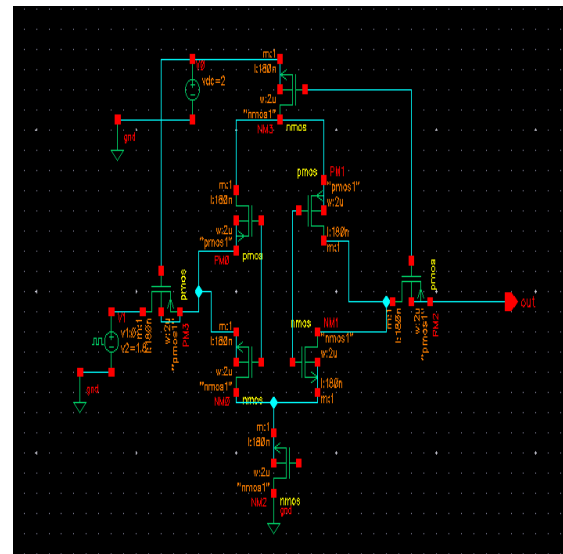


**Fig.2. proposed tail comparator for tri state module**

Adaptation is controlled by the common-mode input voltage: the common source voltage will follow; so raising enables adaptation by increasing the gate-to-drain and source-to-drain electric fields thus attracting hot electrons onto the floating gate. Conversely lowering disables adaptation by decreasing the source-to-drain and gate-to-drain electric fields so that fewer hot electrons are generated and so that fewer hot electrons are collected on the floating gate. During adaptation negative charges accumulate on each of the floating gates, lowering their gate-to-drain and source-to-drain voltages and establishing negative feedback between the outputs and the inputs to achieve stable adaptation.

While the adaptation mechanism for the AFGC results in reduction in the common-mode voltage on the floating nodes, all results reported in this work include any additional error resulting from this shift; thus it does not present a significant limitation to accurate and automatic adaptation. In methods of injection, a static method and a dynamic method. The static method is simple and serves to illustrate the mechanism of calibration, built accuracy is limited in practice. The dynamic injection method overcomes the accuracy limitations of the simple static method and provides calibration accuracy under 1 mV; however, during dynamic injection the adaptation occurs during the evaluation phase so the output of the comparator is latched. This means that the update direction cannot change during a single cycle, thus accurate calibration must be achieved over many clock cycles. We also discuss the inherent tradeoffs between speed and accuracy, which can be tuned using the clock voltage. We present Monte Carlo simulations and experimental results which demonstrate the efficacy of calibration using the dynamic injection method.

**ALGORITHM**

**Step 1: Analyze the circuit for the power conversion for n number of circuit.**

$$(Ck)^n = \sum_{i=0}^n \binom{nC1}{kCn} x m^k C k a^{n-1}$$

**Step 2: Determine the number of conversions to take place and transistors to be used in the conversion process**

$$(nKt)^n = 1 + \frac{tnx}{n1!} + \frac{tn(rn - t1)x^2}{n2!} + \dots$$

**Step 3: Register cells in the path along with the voltage converter are taken and external charge storage devices are taken**

**Step 4: Along with the voltage converter the device for the conversion are attached with the memory cells in the read path**

**Step 5: to the readpath the voltage converter the frequency range is to be set in the input devices.**

**Step 6: pulse input is given as input to the device, and DC voltage are taken for the references.**

**A. Static Injection Method**

The static injection method accomplishes adaptation by applying a constant voltage bias to the clock terminal. When the clock is high, the comparator becomes an amplifier whose differential inputs and differential outputs are related by a finite voltage gain. The constant is the capacitance ratio, where is the capacitance between nodes, and is the total capacitance coupled to the floating node. The voltage gain from floating nodes and to the differential outputs is greater than the overall voltage gain. The goal of offset cancellation is to balance the differential output when the input difference is zero. Suppose that mismatch causes the output to be unbalanced when the inputs are equal. When  $V_{dd}$  is sufficiently high, injection occurs when the common-mode input voltage is raised. Since the source-to-drain voltage of is greater than that of , the injection current onto the floating gate of will be greater than the injection current at and the floating-gate potential will decrease faster than . As a result, the differential current will increase with a concomitant decrease in  $V_{dd}$ , causing the output voltage to rise and to fall. This feedback cycle will drive the floating-gate voltages and to values that compensate for the initial device mismatches. The input-referred offset after calibration depends on early voltage, voltage gain and mismatch of both device and injection parameters. The load operation in the system,

$$Y \alpha + \text{load } \beta = 2 C \frac{1}{2} (\alpha r + \beta) C x \frac{1}{2} (\alpha - \beta r)$$

**Dynamic Injection on the Floating Gates**

We describe a dynamic injection technique which overcomes the overshoot problem observed when using static injection. The dynamic technique achieves

injection during the evaluation phase when the clock signal is low and the comparator is latched, with adaptation achieved over many evaluation cycles. By injecting with a running clock, we use the outcome of each comparison to correct offset during the corresponding evaluation cycle. Thus, the feedback loop encompasses all mismatch and offset within the circuit, and accurate offset cancellation can be achieved. We bias the common-mode input voltage so that the drain-to-channel voltage is insufficient for injection during the reset phase of the clock cycle, but sufficient to produce injection during the evaluation phase when one of the outputs or is close to ground.

**Trade-offs Between Resolution and Speed**

Since offset resulting from device mismatch can be cancelled, the resolution of the AFGC is determined by the input-referred noise. For perfectly calibrated devices, the error introduced by this noise will be random and may be reduced by examining the comparator's outcome over many evaluation cycles. When the devices are not perfectly calibrated, the residual offset contributes an additional source of input-referred noise which is deterministic. Under realistic conditions, this deterministic noise is smaller than the random noise (see above). The relative magnitudes of the deterministic and random noise sources are determined by the injection mismatch ratio. The power of the controller is determined by

$$P = V_0 + I r + m$$

**CIRCUIT DESCRIPTION**

The circuit of the proposed comparator is shown in Fig. 3. In contrast to the conventional comparators latch used in Fig. 1, where only N0 and N1 are initially on, the latch of the proposed comparator is expanded into two paths between the supply rails (transistors N0, N1, P0, P1, P4, and P5), so that, at the beginning of the comparison phase, where both output nodes have the initial condition  $OUT = \overline{OUT} = V_{CO}$  (initially, internal nodes  $FB = \overline{FB} = V_{SS}$ ), transistors N0 and N1 are turned on. However, transistors P0 and P1 are also turned on and build, with input transistors N2 and N3, an amplifier with a distinct working point, which, in contrast to that in Fig. 3, which shows the overall schematic of the module, contributes enough gate-source voltage to transistors N0 and N1 at lower supply voltages. Complete positive feedback of the latch starts when one output node is discharged enough to turn on P4 or P5.

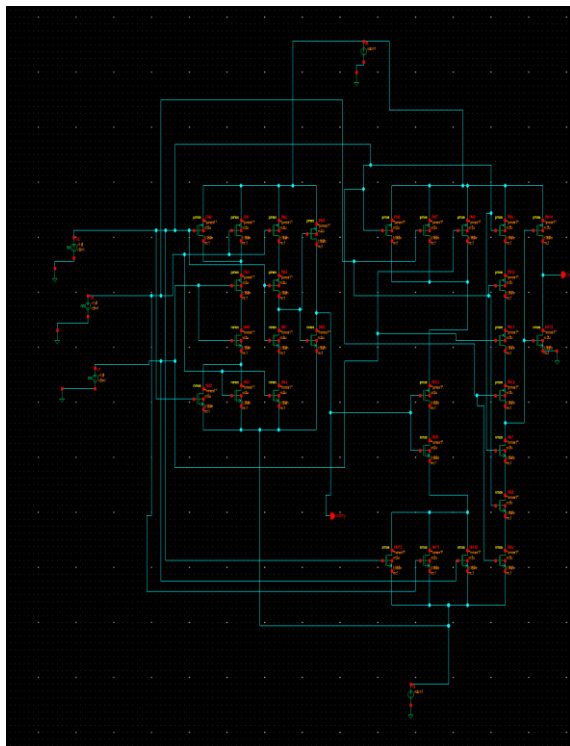


**Fig.3. Proposed schematic of the comparator**

Regeneration is done with N0, N1, P0, and P1, where P4 and P5 help with additional amplification. To get a rail-to-rail output swing and no static power consumption of the comparator, one of the initial load transistors P0 or P1 is switched off, when, during regeneration, FB or FB, respectively, is charged to VCo. The other advantages of a high-impedance input and no direct influence of parasitic capacitances of N2 and N3 to the output nodes are kept. The corresponding transient simulation of Fig. 6 can be seen in Fig. 7. A clock period is divided into two phases: The reset phase (CLK = VSS) is used to establish the initial condition OUT = OUT = VCo for the following comparison phase. (CLK = VCo, VCo is the positive supply voltage of the comparator.) During reset, transistor N6 is switched off, and transistors P2, P3, N4, and N5 are on.

A carrier is described by

$$V = V_c \sin(\omega_c t + \theta)$$

$$v = \{V_c + V_m \sin(\omega_m t)\} * \sin(\omega_c t)$$

**Active Diode**

Fig. 4 shows the schematic of a comparator consisting of a tristate system with a PMOS. In this specific implementation, the drain and source terminals are equivalent to the anode and cathode terminals of a diode. The comparator monitors the voltage between the two terminals. When the anode voltage is higher than the cathode, the comparator outputs a low voltage to the gate terminal to turn ON the PMOS. Otherwise, a high output will be generated to turn OFF the PMOS. In this manner, the active diode behaves as an ideal diode. The

conduction voltage drop of the PMOS is much smaller than the forward-bias voltage drop of a junction diode, and the on-resistance is usually smaller, too. Also, the leakage current in the OFF state can be much smaller than reverse leakage of a junction diode. Despite these advantages, there are several drawbacks with an active diode. First, external supply voltage and power is required for the comparator. In an energy harvesting system, this requires a continuous supply of energy from the source or load, as well as a mechanism for self-starting (bootstrapping) from a completely discharged state. Fortunately, the power consumption is quite low; comparators with <1 μW static power consumption are readily available from commercial vendors, and even lower power comparators may be designed by eliminating unnecessary functions found on commercial ICs. These issues are further discussed in the following. Another drawback of the active diode is that the ON and OFF state of the PMOS is controlled by the differential voltage between its gate and source. Since the source terminal is on the signal path with a volatile potential, a floating control is required, which requires careful design because the control voltage (VGS) is also influenced by the input signal.

**Voltage Doubler Using Active Diodes**

The active diode is configured as a voltage doubler. The circuit consists of a positive and a negative peak detector, generating dc voltages that track the positive and negative peaks of the input. Therefore, a dc voltage of twice the input amplitude can be obtained. When active diodes are used, the conduction voltage drop is much smaller than junction diode, and the circuit can operate at very low input voltage amplitude. While the power requirements for the active diode are expected to be small, the source of the external power must still be considered. A complete energy harvesting system can be expected to have an energy storage unit (e.g., rechargeable battery), as shown in Fig. 3. Here, the battery load provides voltage supply to the comparators in the voltage doubler to enable ac/dc rectification. The input ac voltage is rectified to a dc voltage that is twice the ac amplitude. The low dc voltage is then boosted by a boost converter to a voltage level sufficient to charge the battery. As long as the charging current is higher than the supply current of the comparators, the battery can be charged. In practice, a limit on the battery discharge could be set, so that there would always be sufficient charge and voltage for the active diode operation. This system configuration is plausible by using commercially available ultralow-power comparators and low-voltage boost converters. For example, the comparator used in this paper can work with supply voltage/current of 2.5 V/560 nA [13]. An ultralow-voltage boost converter LTC3108 from Linear Technology can provide an output voltage of 2.35 to 5 V with only 20 mV of input voltage [14]. Additionally,

several other academic efforts have aimed to reduce the input voltage and increase the efficiency of boost converters for energy harvesting applications [15], [16]. Note that in this design, the source terminals of both MOSFETs are connected to the capacitors. Such arrangement helps to reduce the volatility of the source potential. Also, if the comparator power supply terminals are connected to the positive/negative output terminals of the voltage doubler, and the input voltage is high enough, the comparators may function without an external power supply. Under these conditions, the power feedback mechanism shown in Fig. 2 could be eliminated. This input-powered functionality is verified in Section III-D.

For complex  $Z=X+i*Y$ ,  $EXP(Z) = EXP(X)*(COS(Y)+i*SIN(Y))$ .

```
x = [0:pi/36:2*pi];
y = cos(x);
plot(x*180/pi,y)
xlabel('x(degree)'), ylabel('cos(x)')
```

### Circuit Dynamics

The dynamics of the circuits are analyzed to help select component parameters, so that proper functionality and high efficiency can be achieved. As the basic building block of the voltage doubler, the active-diode-based peak detector is analysed to provide insight into the whole circuit. The steady-state open-circuit voltage of the peak detector is calculated with comparator hysteresis taken into consideration.

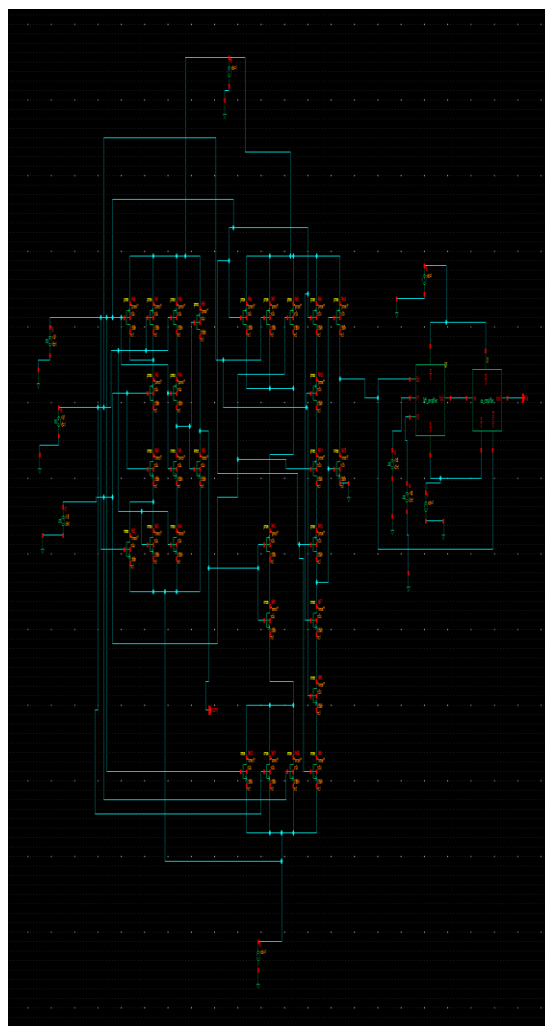


**Fig.4. overall proposed comparator circuit**

### Comparator Hysteresis:

An ideal comparator has perfect zero-crossing detection function; however, typical comparators have hysteresis that creates some small error. Some comparators even intentionally add hysteresis to reduce sensitivity to noise. For active-diode application, since the differential input voltage of the comparator is the product of the drain to source current and on-resistance of the MOSFET, the voltage is usually very small. In order to detect the small input signal, the comparator hysteresis should not be too large. In Cheng et al.'s previous work [12], comparators with a hysteresis band of  $\pm 2$  mV were used, and the output did not reach steady state until a stabilization network was added. To understand the effect of hysteresis, two cases (MOSFET turning ON and MOSFET turning OFF) are considered in the following. First, when the MOSFET is initially turned OFF, the comparator should be able to turn ON the MOSFET when the source voltage is higher than the voltage on the capacitor. Ideally, the MOSFET will turn ON as long as the source voltage is higher than the capacitor voltage by an infinitesimal amount, so that the capacitor voltage should precisely track the peak. However, the differential voltage has to exceed the comparator hysteresis voltage in order to turn ON the

MOSFET. This is illustrated in Fig. 4. In the extreme case, if the initial capacitor voltage is too close to the maximum voltage of the source, the MOSFET will never turn ON, and the peak will be missed, as shown in Fig. 4. Second, if the MOSFET is initially ON, it needs to be turned OFF whenever the source voltage is lower than the voltage on the capacitor (or current reflow is detected).

$$y = -2.5 * a : .05 * a : 2.5 * a;$$

$$XMA2 = (X - a).^2; XPA2 = (X + a).^2; Y2 = Y.^2;$$

$$FCXY = c * ((Y ./ (XMA2 + Y2)) - (Y ./ (XPA2 + Y2)));$$

However, because the minimum detectable voltage exists, the MOSFET will not turn OFF until the capacitor voltage is already higher than the source voltage by a finite value. This is illustrated in Fig. 5. As an extreme case, if the maximum voltage difference between the capacitor and the source is smaller than the minimum detectable voltage, the MOSFET will never turn OFF, and the capacitor voltage will just follow the source, as shown in Fig. 5. It seems obvious that a comparator with no hysteresis will provide optimum solution. In reality, however, a certain degree of noise rejection is sometimes desirable, since the comparator output oscillation due to noise will increase the power consumption. Therefore, a small hysteresis voltage may be desirable, as long as the stability of the circuit can be maintained. This is further studied in the next section.

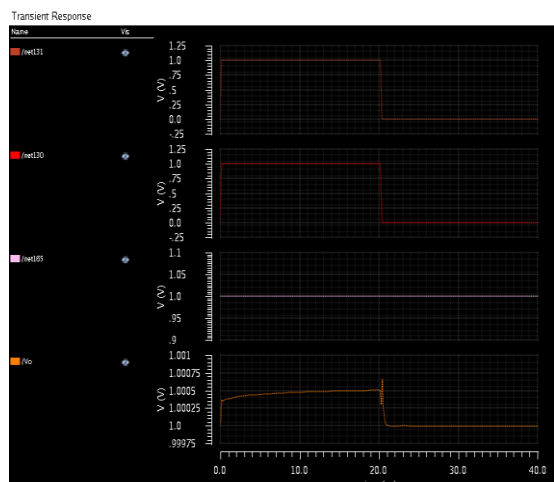


**Fig.5. Transient analysis Active-Diode-Based Peak Detector Open-Circuit Steady-State Capacitor Voltage Analysis:**

In order to determine hysteresis voltage can be tolerated; an analytical solution of the open-circuit steady-state waveform is derived for an active diode-based peak detector (one half of the voltage doubler circuit). The circuit variables are labelled in Fig. 6, and the analysis is based on the following assumptions. The source waveform is given by  $v_{in}(t) = V_{in} \sin(\omega t)$ , and the static voltage on the capacitor is  $V_{c0}$  before the MOSFET is ON. The voltage doubler was built and tested using discrete components to demonstrate and characterize the design concept.

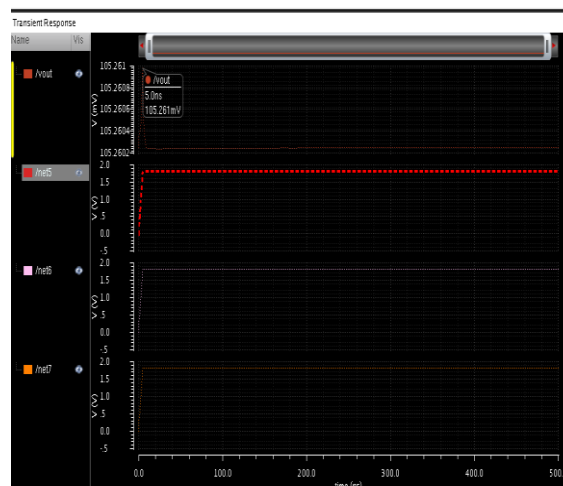


**Fig.6. Transient analysis -2**

Transient analysis are analysed with the proposed comparator. Different voltages are applied over the proposed converter, for the 0.8V input voltage 204.65mV is produced as an output with the reduced low voltages under the high throughput with the less power consumption to the devices. Two different transient analysis are used for the physical comparisons states between the two proposed tri state comparators.

**Open-Circuit Measurements**

Before applying a load, the open-circuit waveform was first measured under different amplitudes and frequencies. With 20 Hz sinusoidal input, the circuit exhibited minimum input voltage amplitude of 5 mV. This lower bound was the point, where the output voltage and input amplitude differed by ~10%. A frequency swept was also performed with 0.25 V amplitude sinusoidal input from 1 to 500 Hz. As the frequency increased, the output waveform started to be distorted.

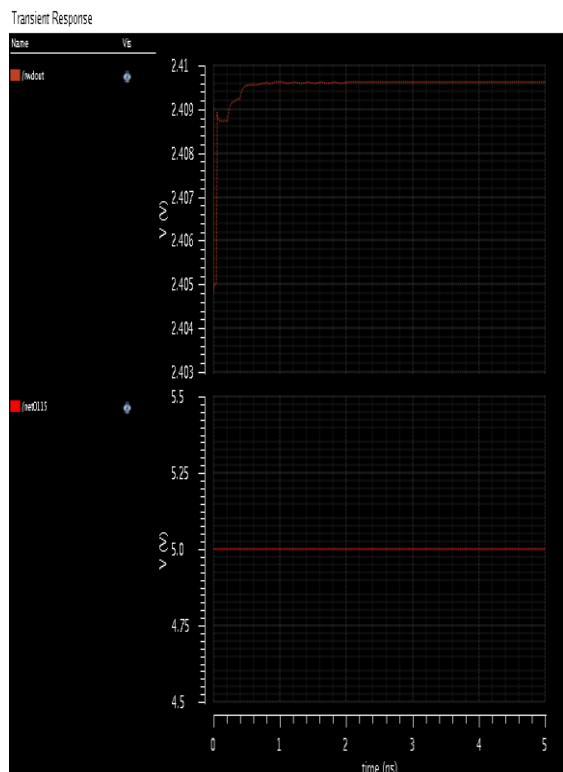


**Fig.7. Transient analysis -3**

**Efficiency and Power Measurements**

Using a pulse input waveform, the measured efficiency for different input amplitudes and different load resistances is plotted. The power efficiency is calculated by  $\text{Efficiency} = \frac{\text{Load power}}{\text{Input power} + \text{External power}} \times 100\%$ . (12) Greater than 80% efficiency was achieved for input voltage amplitudes higher than 0.25V for load resistances from 100Ω up to 5 kΩ. Also note that the efficiency was not sensitive to the input voltage amplitude for voltages between 0.25 to 1.2 V (~10% variation). A possible explanation is as follows. When the input voltage increases, two things happen.

**TABLE I:**

	<b>Proposed Dynamic Comparator</b>	<b>Dynamic Comparator [1]</b>
Technology CMOS	180 nm	180 nm
Supply voltage (V)	0.8	0.8
Maximum sampling frequency	3.4 GHz	2.4 GHz
Delay	246	294
Energy per conversion	0.20p	0.24p
Estimated area	22 μ × 10 μ	28 μ × 14 μ

First, the voltage magnitude on the capacitors (MOSFET source terminals) increase, and the gate to source voltage of the MOSFETs decrease, resulting in increased on-resistance of MOSFETs and decreased

loadpower/input power ratio. Second, the absolute input power is increased and the fixed comparator power consumption becomes less important, which tends to increase the overall efficiency. The combined result of these two contradicting effects makes the overall efficiency less sensitive to input voltage. Under the same testing conditions, the output power is plotted in Fig. 7. The extracted output power ranged from microwatts to tens of milliwatts, scaling approximately proportional to the input voltage squared. The maximum power was consistently achieved at 100 Ω, regardless of the input voltage. This is close to the output impedance of the circuit when both MOSFETs are OFF (~130 Ω). This makes it more convenient to perform impedance matching at the next stage.

**CONCLUSION**

In this work, a comprehensive delay analysis for clocked dynamic comparators along with the new comparator design for functioning with the processor is designed. Two common structures of conventional dynamic comparator and conventional double-tail dynamic comparators with the special multi comparator are designed with the reduced area were analyzed. Also, based on analyses a new dynamic comparator with low-voltage low-power capability was proposed in order to improve the performance of the comparator. Post-layout simulation results in 180nm CMOS technology confirmed that the delay and energy per conversion of the proposed comparator is reduced to a great extent in comparison with the conventional dynamic comparator and multi-tail comparator.

**REFERENCE**

[1] Samaneh Babayan-Mashhadi, and Reza Lotfi, "Analysis and Design of a Low-Voltage Low-Power Double-Tail Comparator", IEEE Transactions On Very Large Scale Integration Systems, Vol. 22, No. 2, February 2014

[2] S. U. Ay, "A sub-1 volt 10-bit supply boosted SAR ADC design in standard CMOS," Int. J. Analog Integr. Circuits Signal Process., vol. 66, no. 2, pp. 213–221, Feb. 2011.

[3] L. Mateu and F. Moll, "Review of energy harvesting techniques and applications for microelectronics," in Proc. SPIE, 2005, pp. 359–373.

[4] Perpetuum Ltd. <http://www.perpetuum.com/>, accessed Mar. 3, 2010.

[5] Ferro Solutions Inc. <http://ferrosi.com/>, accessed Mar. 3, 2010.

[6] Adaptive Energy LLC. <http://www.adaptiveenergy.com/>, accessed Mar. 3, 2010.

[7] J. A. Paradiso and T. Starner, "Energy scavenging for mobile and wireless electronics," IEEE Pervasive Comput., vol. 4, no. 1, pp. 18–27, Jan.–Mar.2005.

[8] J. R. Farmer, "A comparison of power harvesting techniques and related energy storage issues," Master thesis, Virginia Polytechnic Inst. State Univ., 2007.

[9] S. Roundy, P. K. Wright, and J. M. Rabaey, Energy Scavenging for Wireless Sensor Networks: With Special Focus on Vibrations. Springer, 2004, pp. 193–219.

[10] C. Peters, D. Spreemann, M. Ortmanns, and Y. Manoli, "A CMOS integrated voltage and power efficient AC/DC converter for energy harvesting applications," J. Micromech. Microeng., vol. 18, pp. 104005–104013, 2008.

[11] Y. H. Lam, W. H. Ki, and C. Y. Tsui, "Integrated low-loss CMOS active rectifier for wirelessly powered devices," IEEE Trans. Circuits Syst. II, Exp. Briefs, vol. 53, no. 12, pp. 1378–1382, Dec. 2006.

[12] S. Cheng, Y. Jin, Y. Rao, and D. P. Arnold, "A bridge voltage doubler AC/DC converter for low-voltage energy harvesting applications," in Ech. Dig. 9th Int. Workshop Micro and Nanotechnology Power Generation Energy Convers. Apps., 2009, pp. 25–28.

[13] TLV3702 Datasheet, Texas Instruments Inc., Dallas, TX, 2001.

[14] LTC3108 Datasheet, Linear Technology Corp., Milpitas, CA, 2010.

### Author Profile



**Divya Selvan** completed Bachelor of Engineering in Electronics and Communication Engineering from Dr.N.G.P. Institute of Technology, Coimbatore and currently pursuing Master of Engineering in VLSI Design from Karpagam University. Research interest includes low power.